Magnetic ground state of the $M_{n+1}AX_n$-phase nitride Cr_2GaN

Z. Liu, T. Waki, Y. Tabata, K. Yuge, and H. Nakamura*
Department of Materials Science and Engineering, Kyoto University, Kyoto 606-8501, Japan

I. Watanabe
Advanced Meson Science Laboratory, RIKEN Nishina Center, Wako, Saitama 351-0198, Japan
(Received 19 July 2013; revised manuscript received 11 September 2013; published 1 October 2013)

Aiming to find magnetic states in the $M_{n+1}AX_n$ phases, we measured the magnetic susceptibility, the resistivity, and nuclear magnetic resonance of Cr_2GaX (X = N and C). Zero-field and longitudinal-field muon spin relaxation experiments were also applied to Cr_2GaN. A magnetic phase transition, most probably to the spin-density-wave (SDW) state, has been found in Cr_2GaN at $T_N = 170$ K in contrast to the Pauli paramagnetism in the carbide counterpart Cr_2GaC. The origin of the SDW transition is interpreted in terms of possible Fermi-surface nesting in the two-dimensional-like electronic structure.

DOI: 10.1103/PhysRevB.88.134401 PACS number(s): 75.10.Lp, 75.30.Fv, 76.60.−k, 76.75.+i

I. INTRODUCTION

To design magnetic functions in the $M_{n+1}AX_n$ (MAX) phases is a challenging attempt to extend possible applications of the unique nanolaminate. The MAX phases (space group: hexagonal $P6_3/mmc$), where M is an early transition metal, and A an A group element (usually IIIA and IVA), X = N, C, and n = 1,2,3, . . ., attract much attention of many researchers because the characteristic layered structure, in which nets of a metal carbide or nitride, M_6X, interleaved with A-element layers, provides the materials with a unique combination of both metallic and ceramic characters.[1–3] *Magnetic* MAX phases are attractive in the viewpoints of both application and fundamental sciences. The interlayer exchange coupling in the multilayered structure is promising for spintronics applications via, for example, possible giant magnetoresistance. The magnetism realized in the geometrically frustrated two dimensional plane is also intriguing in the field of metallic magnetism. Actually, the possible realization of the spin polarization in some MAX phases, such as Cr_2AlC,[4–6] Cr_2GeC,[7,8] hypothetical $Fe_{n+1}AC_n$,[9] and $(Cr_{1-x}Mn_x)_2AlC$,[10] has been discussed theoretically. Experimental efforts to synthesize $(Cr_{1-x}Mn_x)_2AlC$ (Ref. 11) and $(Cr_{1-x}Mn_x)_2GaC$ (Ref. 12) have been reported. Finally, the room-temperature ferromagnetism has been discovered in $(Cr_{1-x}Mn_x)_2GeC$ just recently.[13]

As above, most of the works on the *magnetic* MAX phases concentrated on carbides. On the other hand, in the field of magnetism, it is well known that the exchange correlation is often enhanced in nitrides.[14] In the present study, to shed light on fundamental properties of the MAX-phase nitrides, we particularly pick up Cr_2GaN with the Cr_2AlC-type structure (Fig. 1), which is only one MAX-phase chromium nitride whose synthesis has ever been reported, and characterize its magnetic properties. In this article, we report an observation of the spin-density-wave (SDW) state in Cr_2GaN. For comparison, the Pauli paramagnetism of the carbide counterpart Cr_2GaC is also presented.

II. EXPERIMENTAL PROCEDURES

Polycrystalline samples of Cr_2GaC and Cr_2GaN were synthesized by solid-state reactions in evacuated quartz tubes. The synthesis of Cr_2GaC was started from a mixture of Cr, C, and Ga powder and heated at 1000 °C for 24 h. The nitride, Cr_2GaN, was made from a mixture of Cr_2N and Ga at 740 °C for 5 h. To obtain single phases of the objective compounds, we optimized the initial Ga content through a trial and error process. As a result, we added excess Ga of ∼10%. Lattice parameters obtained from x-ray diffraction analyses at room temperature agree well with those reported in literature.[15,16] For Cr_2GaN, we performed the Rietveld refinement analysis of the room-temperature x-ray diffraction pattern using RIETAN-2000[17] and obtained lattice parameters $a = 2.883$ and $c = 12.753$ Å and the z coordinate of the Cr position ($4f$ site) $z = 0.0860$. The z value was found to be slightly larger than that predicted in calculations, 0.081–0.082,[18] but comparable to that for Cr_2GaC, 0.08653.[16] The magnetic susceptibility was measured by a SQUID magnetometer (MPMS, Quantum Design), installed at the Research Center for Low Temperature and Materials Sciences, Kyoto University, in the temperature range of 2–300 K. Temperature dependences of the resistivity were measured for pellets sintered from powder by the conventional four-probe method in 5–300 K. Nuclear magnetic resonance (NMR) measurements were performed by a homemade phase-coherent-type pulse spectrometer. For the measurements, fine particles of the samples are soaked in paraffin to fix crystal axes at random. Spin-echo intensity was integrated and recorded as a function of external field to obtain spectra at 4.2 K. Zero-field (ZF) and longitudinal-field (LF) muon spin relaxation (μSR) measurements were made at the RIKEN-RAL Muon Facility[19] at the Rutherford-Appleton Laboratory in the UK using a pulsed positive surface muon beam at 20–300 K. To evaluate the electronic state of Cr_2GaX, first-principles calculations were performed using the plane-wave projector augmented-wave method and the Perdew-Burke-Ernzerhof generalized gradient approximation as implemented in the VASP code.[20]

III. RESULTS AND DISCUSSION

A. Susceptibility and resistivity

Figure 2 shows temperature dependences of the susceptibility for Cr_2GaX. For the carbide, except at a low-temperature

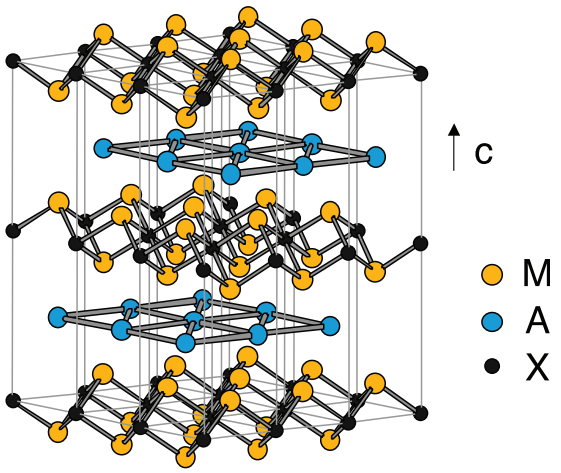

FIG. 1. (Color online) Crystal structure of M_2AX (Cr_2AlC type, $3 \times 3 \times 1$ unit cells), where M_6X nets are interleaved with A-element layers.

part, the susceptibility increases slightly with temperature. This weak temperature dependence is typical for the Pauli paramagnet, indicating that Cr_2GaC is a simple metal in the viewpoint of basic magnetism. The low temperature upturn is ascribed to paramagnetic impurities. We have also measured the susceptibility of other Cr-based carbides, Cr_2AlC and Cr_2GeC, and observed similar temperature dependences, suggesting that known Cr_2AC-type carbides are commonly Pauli paramagnetic. On the other hand, the susceptibility of the nitride Cr_2GaN is characteristic. First, absolute values are larger by about twice, indicating exchange enhancement in the nitride. Second, a reduction is clearly seen below ~170 K, suggesting the occurrence of a phase transition. No temperature hysteresis was observed at the anomaly within the experimental resolution. Since the susceptibility of the metallic magnet is proportional to the density of states at the Fermi level, $D(E_F)$, the reduction of the susceptibility implies a band-(pseudo)gap opening at the Fermi level, E_F.

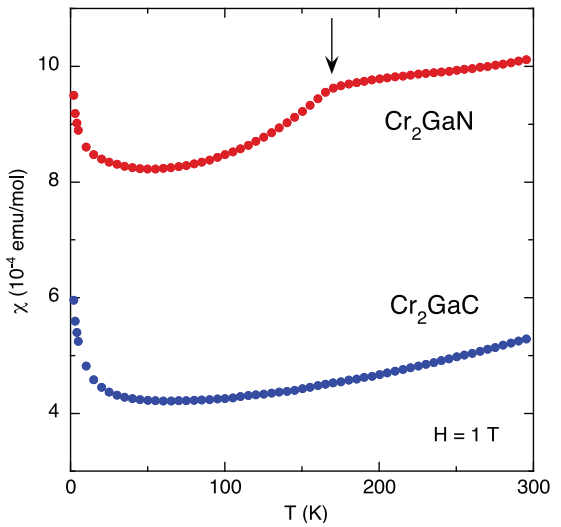

FIG. 2. (Color online) Temperature dependences of the susceptibility for Cr_2GaN and Cr_2GaC measured under a field of 1 T. The arrow indicates the anomaly corresponding to T_N.

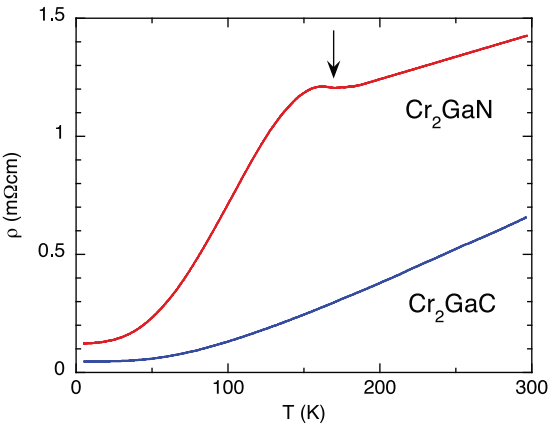

FIG. 3. (Color online) Temperature dependences of the resistivity for Cr_2GaN and Cr_2GaC. The arrow indicates the temperature at which the susceptibility shows the anomaly.

Temperature dependences of the resistivity are shown in Fig. 3. Both Cr_2GaC and Cr_2GaN show metallic behaviors. The resistivity of the carbide shows a monotonic temperature dependence, indicating no phase transition being in agreement with the data of the susceptibility. On the other hand, the nitride shows an anomalous behavior. At high temperatures, the resistivity is nearly linear with a positive slope like the carbide, increases once slightly below ~170 K to make a small hump, and decreases rapidly at lower temperatures. No temperature hysteresis has been observed. The larger temperature dependence of the nitride suggests the stronger effect of spin fluctuations in the material.

It is reasonable to compare the magnetic and transport properties of Cr_2GaN with those of pure metallic chromium, which is the prototype showing a spin-density-wave (SDW) transition.[21] In fact, the reduction of the susceptibility and the small hump of the resistivity below ~170 K are markedly similar to those observed for pure chromium at the SDW transition,[22–24] although the Néel temperature of chromium is much higher of 311 K. The small hump of the resistivity is interpreted as the combined effect of opening of an energy gap at the transition and the temperature dependence of the relaxation rate at the lower temperatures.[25]

B. ^{69}Ga and ^{71}Ga NMR

We performed microscopic magnetic measurements to detect spin polarization directly in the SDW state. Figure 4 shows Ga spin-echo NMR spectra of Cr_2GaX recorded as a function of external field at a frequency of 38.5 MHz and at 4.2 K. For the carbide, we obtained a well resolved nonmagnetic spectrum, which is interpreted as follows. There are two Ga nuclides in nature, ^{69}Ga and ^{71}Ga[26] (natural abundance: 60% and 40%, respectively; nuclear spin: $I = 3/2$ for both; gyromagnetic ratios: $^{69}\gamma/2\pi = 10.219$ and $^{71}\gamma/2\pi = 12.984$ MHz/T; the ratio of nuclear quadrupole moments: $^{69}Q/^{71}Q = 1.587$[27]). The Ga site in these compounds is crystallographically unique ($2d$) and axially symmetric ($\bar{6}m2$), resulting in the nuclear quadrupole interaction with zero asymmetry parameter ($\eta = 0$). In the strong-field condition, we expect to observe a pair of first-order quadrupolar satellites

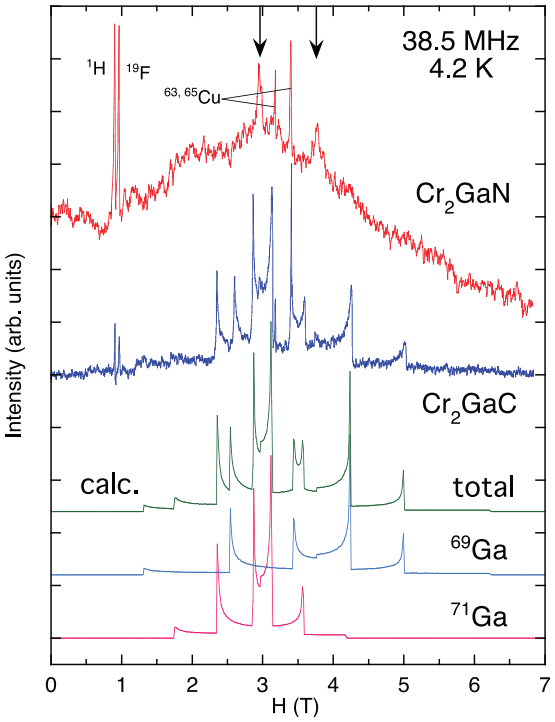

FIG. 4. (Color online) Field-swept ^{69}Ga and ^{71}Ga NMR spectra for Cr_2GaN and Cr_2GaC measured at a frequency of 38.5 MHz and at 4.2 K. Arrows indicate zero shift positions for ^{69}Ga and ^{71}Ga. Simulated paramagnetic powder-pattern spectra are also presented for comparison. Nuclear quadrupole frequencies, 25.1 and 15.8 MHz, were assumed for ^{69}Ga and ^{71}Ga, respectively. The hyperfine shift was neglected for simplicity.

and a center line for each nucleus. In the bottom of Fig. 4, computer-generated powder patterns assuming quadrupole frequencies of 25.1 and 15.8 MHz for ^{69}Ga and ^{71}Ga, respectively, are presented. These relatively large quadrupole frequencies reflect the anisotropic nature of the nanolaminate structure. Here we neglected a possible hyperfine shift, for simplicity. In this condition, the center lines have characteristic structures split by the second-order quadrupolar interaction. The final calculated pattern, which was drawn taking account of the natural abundance of ^{69}Ga and ^{71}Ga, agrees well with the experimental spectrum of Cr_2GaC, proving unambiguously that the compound is nonmagnetic at the temperature. On the other hand, the spectrum of the nitride at the same temperature is considerably and inhomogeneously broadened. Note that the signal intensity is finite even at zero external field, and that the spectrum is broadened at around zero shift positions. This result, indicating the presence of considerably distributed internal fields from zero to at least a few tesla, is thoroughly consistent with the microscopic description anticipated for the SDW state. However, since the nuclear quadrupolar interaction in Cr_2GaN is expected to be considerably large and comparable to the possible Zeeman interaction, the distribution of only electrical field gradient, which is caused, for example, by a charge-density wave state, cannot be neglected as the origin of the spectral broadening. To exclude such a possibility, we employed another microscopic probe, ZF/LF-μSR, for Cr_2GaN.

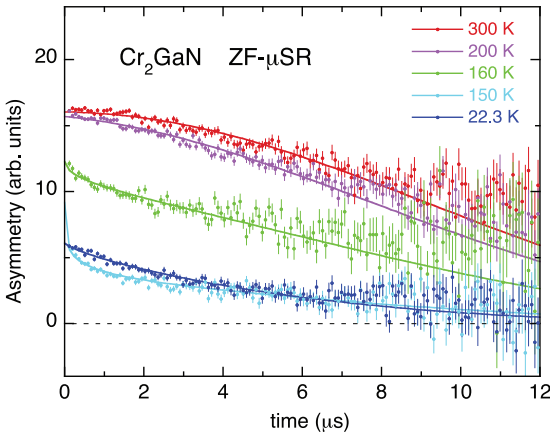

FIG. 5. (Color online) Typical examples of ZF-μSR spectra (at 22.3, 150, 160, 200, and 300 K) of Cr_2GaN. Solid curves indicate the fit by the damped Kubo-Toyabe function.

C. ZF- and LF-μSR

Being different from NMR, μSR probes only the magnetic field, and is very sensitive to the appearance and variation of the internal field. Typical examples of ZF-μSR spectra are shown in Fig. 5. At high temperatures of 200–300 K, the feature of the relaxation is essentially the same and shows Gaussian-type depolarization. This behavior is attributable to tiny dipolar fields coming from randomly oriented nuclear spins; the static field is $\lesssim 6$ Oe. In the temperature range of 150–200 K, the relaxation curve is drastically changed. The loss of the initial asymmetry is appreciable. This is mainly due to the appearance of fast relaxation. Such a behavior is often observed as a result of magnetic ordering.[28,29] In the present case, the anomaly is reasonably ascribed to the Cr electronic spin dynamics.

To discuss quantitatively, we fit the spectra with the frequently used damped Kubo-Toyabe function as

$$A(t) = A_0 \exp[-(\lambda t)^{\beta}] G^{\mathrm{KT}}(\Delta, t), \qquad (1)$$

with

$$G^{\mathrm{KT}}(\Delta, t) = \tfrac{1}{3} + \tfrac{2}{3}(1 - \Delta^2 t^2) \exp\left(-\tfrac{1}{2}\Delta^2 t^2\right), \qquad (2)$$

where A_0 is the initial asymmetry, Δ/γ_μ the width of the static field distribution (γ_μ the muon gyromagnetic ratio) originating in nuclear spins, λ the damping rate associated with an additional fast relaxation process, and β the stretched exponent in the range of $0 < \beta \leqslant 1$ representing the distribution of the damping rate. In the fitting, we estimated $\Delta = 7.89 \times 10^4$ s^{-1} from high-temperature spectra, and treated Δ as constant in all the temperature range. Figures 6 and 7 show temperature dependences of A_0 and λ, respectively. The inset of Fig. 7 shows the temperature dependence of β. Below $\sim$170 K, A_0 is reduced markedly associated with the critical divergence of λ, and approaches $\sim 1/3$ of the high-temperature value at low temperatures. β also shows singularity below $\sim$170 K. These behaviors apparently indicate critical slowing down of electronic spins below $\sim$170 K.

The nature of the low-temperature state was investigated by LF-μSR. Typical LF-μSR spectra measured under several different longitudinal fields, B, at a temperature of 25 K

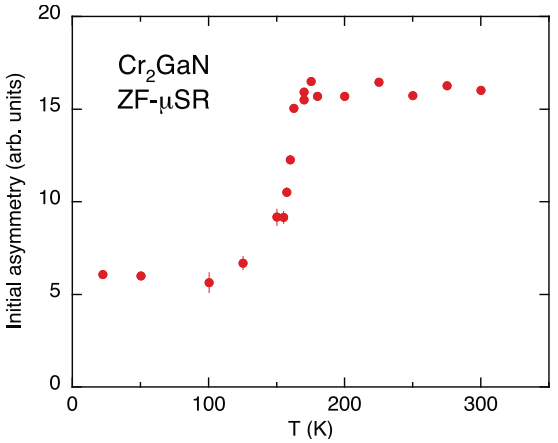

FIG. 6. (Color online) Temperature dependence of the initial asymmetry of the ZF-μSR spectra for Cr_2GaN.

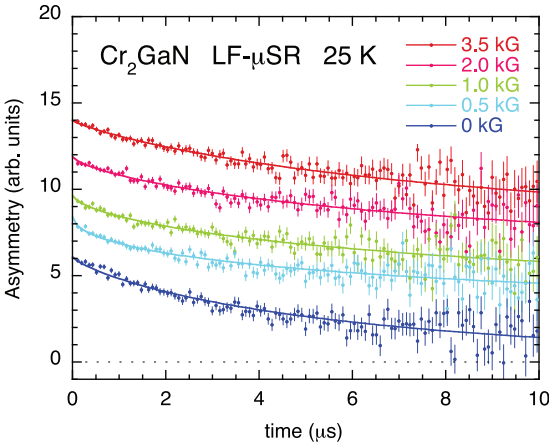

FIG. 8. (Color online) Typical LF-μSR spectra of Cr_2GaN measured at 25 K. Solid curves are the best fits to the stretched exponential function.

are shown in Fig. 8. The asymmetry recovers systematically with increasing B, suggesting that muon spins are decoupled from local and static internal fields, $\boldsymbol{B}_{\rm loc}$, by applying $\boldsymbol{B}$. The muon spin polarization at each B was estimated by fitting the time spectra $A(t)$ to a stretched exponential function $A(t) = A_0 \exp[-(\lambda t)^{\beta}] + A_{\infty}$, where A_{∞} is the longitudinal-field-induced baseline with respect to that at $B = 0$, and by normalizing the initial asymmetry $A(0)$ by the full asymmetry estimated from the ZF spectrum at high temperatures. The normalized initial asymmetry is plotted in Fig. 9 as a function of B. By averaging the sum of $\boldsymbol{B}$ and $\boldsymbol{B}_{\rm loc}$ along the direction of $\boldsymbol{B}_{\rm loc}$, the longitudinal field dependence of the muon spin polarization, namely, the decoupling of muon spins from a unique $B_{\rm loc}$, is generally given by

$$G^{\rm LF}(x) = \frac{3}{4} - \frac{1}{4x^2} + \frac{(x^2-1)^2}{8x^3} \ln\left|\frac{x+1}{x-1}\right|, \qquad (3)$$

with $x = B/B_{\rm loc}$, which has actually been observed in a number of magnetically ordered materials.[30,31] The best fit to this equation, with $B_{\rm loc} = 1.2$ kOe, is indicated by the broken curve in Fig. 9. Our data is deviated somehow from the expected curve. Generally, we expect the continuous

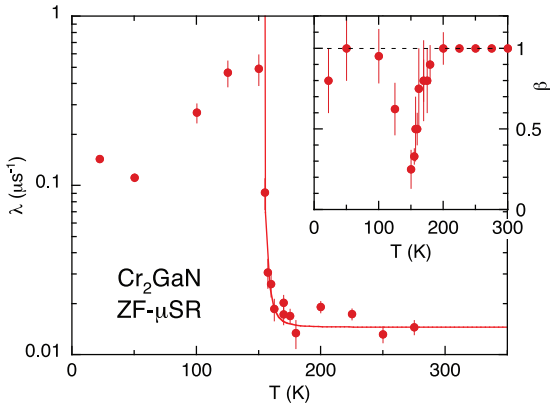

FIG. 7. (Color online) Temperature dependence of the muon-spin relaxation rate λ in Cr_2GaN. The solid curve is the guide for eyes. Inset shows the temperature dependence of the stretched exponent β.

distribution of $B_{\rm loc}$ at interstitial sites in incommensurate magnetic structures in contrast to a unique or fixed $B_{\rm loc}$ in commensurate ones.[32,33] The distribution function of $B_{\rm loc}$ in the former case is generally expressed as

$$P(B_{\rm loc}) = \frac{2}{\pi} \frac{B_{\rm loc}}{\sqrt{\left(B_{\rm loc}^2 - B_{\rm min}^2\right)\left(B_{\rm max}^2 - B_{\rm loc}^2\right)}} \qquad (4)$$

at $B_{\rm min} < B_{\rm loc} < B_{\rm max}$, where $B_{\rm min}$ and $B_{\rm max}$ are minimum and maximum values of distributed $B_{\rm loc}$. In this case, the longitudinal field dependence of the muon spin polarization is expected to be given by

$$G_{\rm ic}^{\rm LF}(B) = \int_0^{\infty} P(B_{\rm loc}) G^{\rm LF}(B/B_{\rm loc})\, dB_{\rm loc}. \qquad (5)$$

The solid curve in Fig. 9 represents a tentative calculation of Eq. (5) with $B_{\rm min} = 0.1$ and $B_{\rm max} = 2.0$ kOe, which reproduces well the trend of the experimental field dependence. Thus the above LF-μSR results, together with the NMR data, are consistent with the static and distributed internal fields

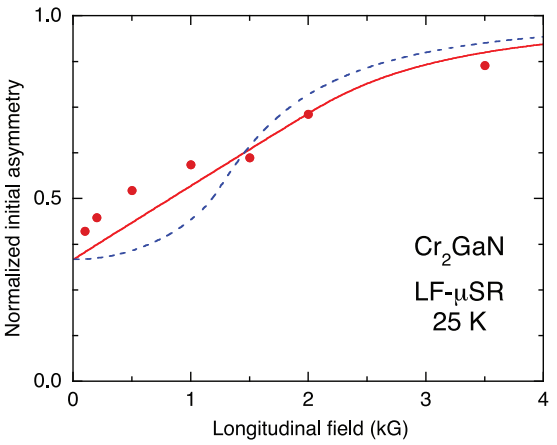

FIG. 9. (Color online) Longitudinal field dependence of muon spin polarization for Cr_2GaN at 25 K. The dotted and the solid curves represent the best fit to Eq. (3) with $B_{\rm loc} = 1.2$ kOe and the calculation assuming Eq. (5) with $B_{\rm min} = 0.1$ and $B_{\rm max} = 2$ kOe, respectively.

expected for the incommensurate SDW state, and rule out possibilities of simple antiferromagnetic structures such as those discussed for Cr_2AlC in Ref. 6. The value of the ordered magnetic moment is not easily estimated but would be in a range of 0.1–1 μ_B/Cr judging from the internal fields. Neutron diffraction experiment, which provides us the information on the magnetic modulation vector too, is desirable.

D. Electronic structure calculations

Here we try to discuss the origin of the SDW transition. Electronic structure calculations have already been reported for Cr_2GaC[18] and Cr_2GaN[34] independently. In the present study, we performed band structure calculations for the spin-unpolarized state of both the compounds on the same basis to compare their electronic states to discuss mainly the Fermi surface topology in the paramagnetic state. The calculated results are essentially the same as those in the literature. Here we show only total and partial electronic densities of states in Fig. 10. The difference between the nitride and the carbide is not so significant; in both cases Cr-3*d* bands dominate $D(E_F)$, while Ga and N/C do not.

For the layered compounds, we expect the two dimensional nature of the electronic structure. Figure 11 shows cross sections of Fermi surfaces consist of the 21st band cut in the a^*-b^* plane at three different c^* for both the nitride and the carbide. As seen in the figure, the three cross sections coincide nearly completely, indicating a cylindrical shape of Fermi surfaces. This topological feature strongly suggests that the nesting of the Fermi surfaces causes the SDW formation. One of the possible wave vectors of the Fermi-surface nesting, (0.56,0,0), is indicated by the arrow in Fig. 11. Recently, similar cylindrical Fermi surfaces have been reported for Cr_2GeC,[8] suggesting the common topological feature in the MAX phases.

Here we should note that the cylindrical Fermi surfaces are seen for both the nitride and the carbide. Why does only the nitride show the SDW transition? One of the possible reasons is the different exchange enhancement as anticipated from the magnitudes of the experimental susceptibility. On the other hand, however, the difference in $D(E_F)$ is not so

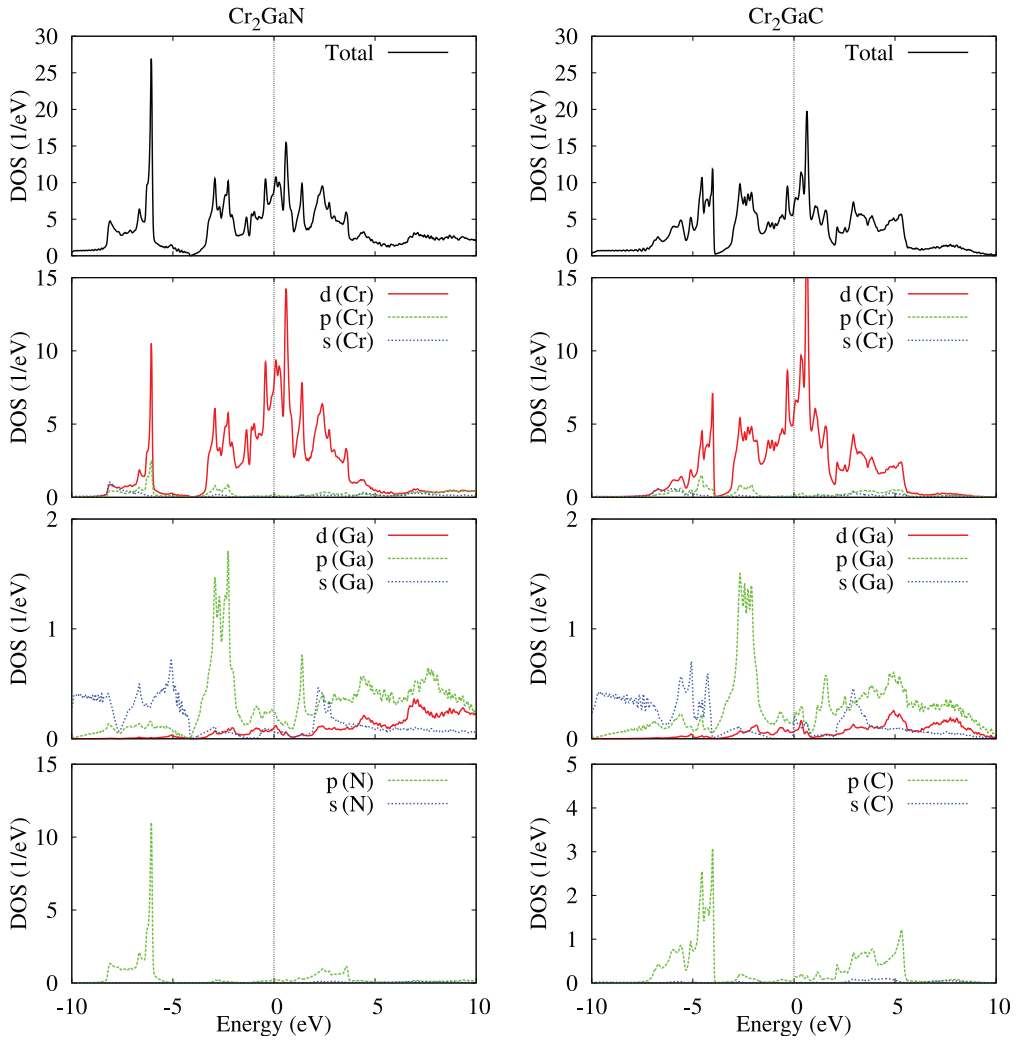

FIG. 10. (Color online) Total and partial density of states of spin-unpolarized Cr_2GaN (left) and Cr_2GaC (right).

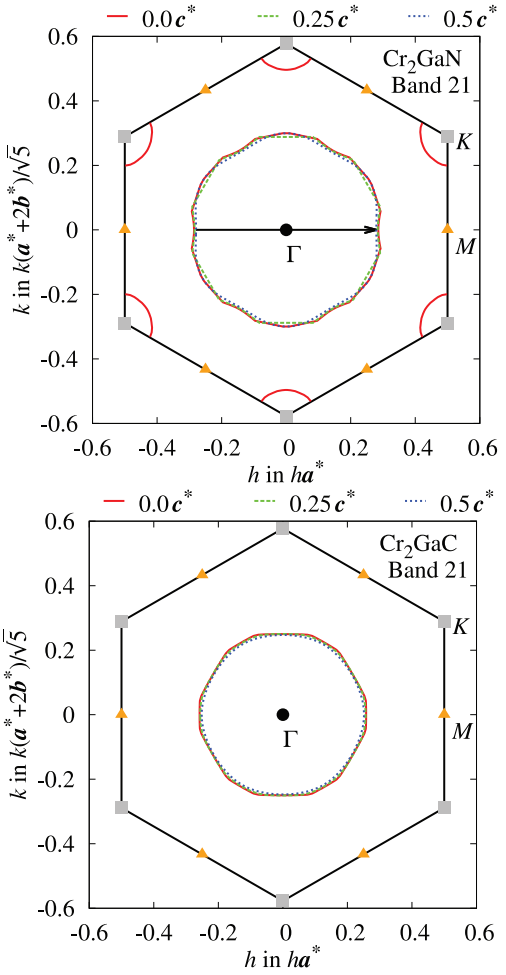

FIG. 11. (Color online) Cross sections of Fermi surfaces consist of the 21st band for spin-unpolarized Cr_2GaN (top) and Cr_2GaC (bottom). The arrow indicates one of possible nesting vectors, (0.56,0,0), in the hexagonal Brillouin zone.

appreciable as in Fig. 10. This is rather reasonable because the crystal structure and the Cr-Cr interatomic distance are nearly the same [the intralayer Cr-Cr distances at room temperature are 2.883 (present study) and 2.9008 Å[16] for the nitride and the carbide, respectively]. Hence the origin of the exchange enhancement may not be straightforward. The most appreciable difference in the band structures is the energy of X-2p bands with respect to E_F. As seen in Fig. 10, the dominant part of N-2p bands (~ -6 eV) is deeper than that of C-2p (~ -4 eV). Since the X atom mediates the electron transfer between Cr atoms belonging to two different layers, the deeper N-2p level may result in better Cr-3d electron confinement in the Cr planes and facilitate the Fermi-surface nesting.

Another possible origin is found in lattice properties. Since the SDW formation is often mediated by the electron-phonon coupling, elastic properties, which are related with covalency between Cr-3d and X-2p, may discriminate the ground state. If the material is elastically soft, the modulated state with an energy gap may be energetically favorable even if the system costs elastic energy. Cui *et al.*[35] performed band calculations of Cr_2AlX (X = N and C), compared elastic properties, and concluded that the nitride is more ductile. This trend is also expected in the case of Cr_2GaX.

IV. CONCLUSION

We have found that the $M_{n+1}AX_n$ phase nitride, Cr_2GaN, shows a SDW transition at $T_N = 170$ K in contrast to the Pauli paramagnetism in the carbide counterpart Cr_2GaC. The NMR and μSR results are totally consistent with the microscopic description expected for the SDW ground state. The formation of the SDW state is interpreted in terms of the nesting of Fermi surfaces of the two-dimensional-like electronic structure. The present study revealed that the MAX-phase nitrides are promising to exhibit electronic ground states.

*nakamura.hiroyuki.2w@kyoto-u.ac.jp

[1]M. W. Barsoum, Prog. Solid State Chem. **28**, 201 (2000).
[2]P. Eklund, M. Beckers, U. Jansson, H. Högberg, and L. Hultman, Thin Solid Films **518**, 1851 (2010).
[3]Z. M. Sun, Int. Mater. Rev. **56**, 143 (2011).
[4]Y. L. Du, Z. M. Sun, H. Hashimoto, and M. W. Barsoum, J. Appl. Phys. **109**, 063707 (2011).
[5]M. Ramzan, S. Lebegue, and R. Ahuja, Phys. Status Solidi RRL **5**, 122 (2011).
[6]M. Dahlquist, B. Alling, and J. Rosén, J. Appl. Phys. **113**, 216103 (2013).
[7]W. Zhou, L. Liu, and P. Wu, J. Appl. Phys. **106**, 033501 (2009).
[8]M. Mattesini and M. Magnuson, J. Phys.: Condens. Matter **25**, 035601 (2013).
[9]W. Luo and R. Ahuja, J. Phys.: Condens. Matter **20**, 064217 (2008).
[10]M. Dahlqvist, B. Alling, I. A. Abrikosov, and J. Rosen, Phys. Rev. B **84**, 220403(R) (2011).
[11]A. Mockute, M. Dahlqvist, J. Emmerlich, L. Hultman, J. M. Schneider, P. O. Å. Persson, and J. Rosen, Phys. Rev. B **87**, 094113 (2013).
[12]S. Lin, P. Tong, B. S. Wang, Y. N. Huang, W. J. Lu, D. F. Shao, B. C. Zhao, W. H. Song, and Y. P. Sun, J. Appl. Phys. **113**, 053502 (2013).
[13]A. S. Ingason, A. Mockute, M. Dahlqvist, F. Magnus, S. Olafsson, U. B. Arnalds, B. Alling, I. A. Abrikosov, B. Hjörvarsson, P. O. Å. Persson, and J. Rosen, Phys. Rev. Lett. **110**, 195502 (2013).
[14]J. M. D. Coey and P. A. I. Smith, J. Magn. Magn. Mater. **200**, 405 (1999).
[15]L. Farber and M. W. Barsoum, J. Mater. Res. **14**, 2560 (1999).
[16]J. Etzkorn, M. Ade, D. Kotzott, M. Kleczek, and H. Hillebrecht, J. Solid State Chem. **182**, 995 (2009).
[17]F. Izumi and T. Ikeda, Mater. Sci. Forum **321-324**, 198 (2000).
[18]A. Bouhemadou, Solid State Sci. **11**, 1875 (2009).

[19]T. Matsuzaki, K. Ishida, K. Nagamine, I. Watanabe, G. H. Eaton, and W. G. Williams, Nucl. Instrum. Methods Phys. Res., Sect. A **465**, 365 (2001).
[20]J. P. Perdew, K. Burke, and M. Ernzerhof, Phys. Rev. Lett. **77**, 3865 (1996).
[21]E. Fawcett, Rev. Mod. Phys. **60**, 209 (1988).
[22]B. C. Munday, A. R. Pepper, and R. Street, in *Proceedings of the International Conference on Magnetism, Nottingham, 1964* (Institute of Physics and The Physical Society, London, 1965), p. 201.
[23]W. B. Muir and J. O. Ström-Oisen, Phys. Rev. B **4**, 988 (1971).
[24]C. Akiba and T. Mitsui, J. Phys. Soc. Jpn. **32**, 644 (1972).
[25]E. Fawcett, H. L. Alberts, V. Yu. Galkin, D. R. Noakes, and J. V. Yakhmi, Rev. Mod. Phys. **66**, 25 (1994).
[26]R. K. Harris, E. D. Becker, S. M. Cabral de Menezes, R. Goodfellow, and P. Granger, Pure Appl. Chem. **73**, 1795 (2001).
[27]M. Pernpointner and P. Schwerdtfeger, Chem. Phys. Lett. **295**, 347 (1998).
[28]I. Watanabe, M. Aoyama, M. Akoshima, T. Kawamata, T. Adachi, Y. Koike, S. Ohira, W. Higemoto, and K. Nagamine, Phys. Rev. B **62**, R11985 (2000).
[29]I. Watanabe, T. Adachi, K. Takahashi, S. Yairi, Y. Koike, and K. Nagamine, Phys. Rev. B **65**, 180516(R) (2002).
[30]I. Watanabe, M. Akoshima, Y. Koike, S. Ohira, and K. Nagamine, Phys. Rev. B **62**, 14524 (2000).
[31]K. Hachitani, H. Fukazawa, Y. Kohori, I. Watanabe, C. Sekine, and I. Shirotani, Phys. Rev. B **73**, 052408 (2006).
[32]D. R. Noakes, Phys. Rev. B **44**, 5064 (1991).
[33]L. P. Le, A. Keren, G. M. Luke, B. J. Sternlieb, W. D. Wu, Y. J. Uemura, J. H. Brewer, T. M. Riseman, R. V. Upasani, L. Y. Chiang, W. Kang, P. M. Chaikin, T. Csiba, and G. Grüner, Phys. Rev. B **48**, 7284 (1993).
[34]Z. J. Yang, R. F. Linghu, X. L. Cheng, and X. D. Yang, Acta Phys. Sin. **61**, 046301 (2012).
[35]S. X. Cui, D. Q. Wei, H. Q. Hu, W. X. Feng, and Z. H. Gong, J. Solid State Chem. **191**, 147 (2012).